Reputation-Based Fair Power Allocation to Plug-in Electric Vehicles in the Smart Grid

Abdullah Al Zishan, Moosa Moghimi Haji, Omid Ardakanian
University of Alberta, Edmonton, AB, Canada
{azishan,moghimih, oardakan}@ualberta.ca

***Abstract*—We present a reputation-based framework for allocating power to plug-in electric vehicles (EVs) in the smart grid. In this framework, the available capacity of the distribution network measured by distribution-level phasor measurement units is divided in a proportionally fair manner among connected EVs, considering their demands and self-declared deadlines. To encourage users to estimate their deadlines more precisely and conservatively, a weight is assigned to a each deadline based on the user's reputation, which comprises two kinds of evidence: deadlines declared before and after the actual departure times in the recent past. Assuming reliable communication between sensors installed in the network and charging stations, we design a decentralized algorithm which allows the users to independently compute their fair share based on signals received from upstream sensors without sharing their private information, e.g., their deadline, with a central scheduler. We prove that this algorithm achieves quadratic convergence under specific conditions and evaluate it empirically on a test distribution network by comparing it with a centralized algorithm which solves the same optimization problem, a decentralized gradient-projection algorithm with linear convergence, and earliest-deadline-first and least-laxity-first scheduling policies. Our results corroborate that the proposed algorithm can track the available capacity of the network despite changes in the demands of homes and other inelastic loads, improves a fairness metric, and increases the overall allocation to users who have a better reputation.**

***Index Terms*—Decentralized Optimal Control, Power Distribution Grid, Reputation-based Service.**

I. Introduction

Electric vehicles (EVs) have become increasingly popular in recent years as they are essential to reduce petroleum dependence and carbon emissions in developed and developing countries [1]. A high penetration of plug-in EVs in distribution networks is anticipated to give rise to several problems, such as transformer overloading, voltage sags, and increased heat losses [2], [3]. This necessitates a demand-side management strategy to control the real power drawn by charging stations, especially as residential and workplace electric vehicle charging stations increase in number. Controlling the EV charging demand is possible due to its *elasticity*, i.e., the charge power of an EV connected to a charging station can be adjusted within certain bounds as long as its battery is charged to a desired level by a deadline [4]. Hence, the EV charging load is characterized with a demand that must be met by a deadline.

To accommodate a higher penetration of EVs safely and efficiently in today's distribution networks, many control methods have been proposed, including centralized methods [2], [5], [6], where a central controller decides on the charge powers of EVs, and decentralized methods [7]–[9], where the control problem is decomposed into several subproblems which are solved by individual charging stations or neighbourhood controllers to determine the charge powers of the respective connected EVs. Nevertheless, existing methods ignore the user-specified deadlines entirely or assume they must be met at all times. The former leads to best-effort service, as in the Internet, which is not be suitable for the power grid.

Incorporating the user-specified deadlines in a scheduling policy is nontrivial. Specifically, prioritizing EV charging according to the user-specified deadlines [10] will only work if there is a well-structured billing mechanism in place, which ensures users with earlier deadlines pay a higher price for electricity. Without such a mechanism, this prioritization opens the door for manipulation in any scheduling problem [11], [12]. For example, users may claim an earlier deadline hoping to receive better service compared to their neighbours. This could strain the distribution grid and increase losses if the deadlines were taken into account without any adjustment. What makes scheduling with deadlines even more challenging is the non-deterministic nature of trips especially in the context of residential charging. Users can at best report their estimated deadline after adding (or subtracting) a value to it, leading to two different types of users: conservative and risk-taking.

This paper addresses how to handle deadlines, fairness, and efficiency requirements simultaneously by proposing a novel framework for EV charging centred around the notion of reputation. We propose a deadline-aware mechanism which takes into account the user's reputation in the recent past, thereby preventing users from gaming the system by claiming false deadlines repeatedly. The reputation comprises two kinds of evidence: deadlines declared prior and past the actual departure times. Furthermore, to minimize the communication overhead and protect user privacy we design a decentralised control algorithm which allows the charging stations to compute their fair share independently based on coordination signals they receive from sensors in the distribution network. Our contribution is threefold:

- We propose a reputation-based mechanism for charging plug-in EVs that fairly allocates charge powers to prevent overloading of substation and distribution transformers;
- We present a scaled gradient-projection algorithm for decentralized control of EV charging and prove that it has super-linear convergence when its parameters are tuned carefully;

- We simulate our method on a test distribution network with real EV data and compare it with different baseline algorithms to show its superior performance and that it favors conservative users.

We make several assumptions in this paper. We assume that every transformer that is likely to be overloaded is equipped with a sensor that measures its loading level, and that these sensors are connected to downstream charging stations via a broadband communication network. Modern distribution grids are being equipped with such monitoring and communication infrastructure [13]. We assume that the sensing nodes have memory to store past behavior of each user and can perform basic arithmetic operations to generate the congestion signal.

II. Related Work

A. EV Charging Scheduling

Optimal scheduling of EV charging has been extensively studied in recent years. The scheduling objectives can be broadly divided into two categories. The main objective of the first category is to provide voltage and frequency support to the grid. For example, [14], [15] focus on voltage regulation using the EV charging load, while [16], [17] focus on providing secondary frequency support to the grid. In the second category, the emphasis is on optimizing some performance metric for PEV owners rather than considering the services that can be offered to the grid. References [18], [19] propose day-ahead scheduling methods to maximize the revenue of EV owners considering electricity prices. A method is proposed in [20] for secondary frequency support, while reducing the battery degradation and maximizing the revenue of EV owner.

The scheduling algorithms can be divided into centralized and decentralized. In centralized algorithms all user data and measurements are sent to a control center which solves an optimization problem and sends back control signals to individual charging stations. For example, centralized scheduling methods are proposed to maintain the voltage profiles [21], to minimize losses in the grid besides improving the voltage profiles [22], and to prevent congestion in the grid [23]. These methods do not scale with the size of the network since the control center is a bottleneck which is responsible for all computation. When there are many sensors and charging stations in the system, there might be congestion in the communication network as well. Furthermore, transmitting data to a control center raises privacy concerns, especially if this data contains EV arrival and departure times.

To overcome these problems, several decentralized methods are proposed in the literature [24], [25]. These methods are compelling when the EV penetration level is high, but they typically suffer from slow convergence in large distribution systems. Reference [14] proposes a decentralized algorithm, i.e., shrunken-primal-dual sub-gradient (SPDS), to improve the demand profile while meeting heterogeneous individual charging requirements of EVs and satisfying distribution grid power quality requirements. This method is a variant of regularized Lagrangian which requires two-way explicit communication and exhibits a slow convergence rate. In [26] a SPDS algorithm is developed for decentralized control. However, this method requires two-way communications between charging stations and operators, whereas the method we propose in this work requires only one-way communication by leveraging local information and the physical system. Moreover, their proposed algorithm is first-order and exhibits linear convergence which is slower than the convergence rate of our algorithm. In [27] authors propose an EV charging controller inspired by the TCP slow start mechanism used in the Internet. The authors use the traffic light model, a congestion notification mechanism to report the status of the grid in real time. However, this method does not solve an optimization problem to establish the optimal control, and therefore fairness is not theoretically guaranteed.

B. Deadline-Aware Scheduling

Incorporating deadlines in scheduling has been extensively studied over the past three decades in the context of real-time scheduling of computer systems, including operating system, distributed systems, and data centers. Reference [28] studies the minimum laxity policy (ML) with multiple processors/servers and the preemptive earliest deadline (ED) policy with a single server, and presents different performance bounds for these policies. In [29], the impatient customers queue model is introduced where jobs (customers) request to complete execution or, at least, reach the server before a given deadline. The problem is modelled as a stochastic recursive sequence that keeps track of all service and patience times of the customers present in the system. The Earliest Progressive Deadline First is proposed in [30] as a class of policies considering server-side job scheduling with progressive deadlines.

However, little work has been done on EV scheduling considering inaccuracies in the reported deadlines. In an expandable service system, variability in service capacity incurs infrastructural and operational costs. To address this problem, an optimization framework is proposed in [31] to reduce service variance while maintaining deadlines and demands of jobs. Although it primarily focuses on cloud services, the authors have considered an EV charging scenario. Our work differs from this work in several ways. First, their proposed method solves the optimization problem once at the beginning of the time horizon based on some statistics about future behavior, whereas our approach is real time and makes decisions based on the currently available information. Second, they assume that the user-specified deadlines are precise, whereas in our model, the specified deadlines may be different from the actual deadlines. The closest work to ours formulates the EV charging control with deadline as a feasibility problem [32]. However, inspired by the best effort service in the Internet, our proposed method uses “soft deadline” which means that it does its best to meet the demand of urgent EVs first. Additionally, we safeguard the system from manipulation that could result from claiming urgency in a deceitful manner.

C. Gradient-Projection Algorithms

The first-order gradient-projection algorithm (GPA) has been applied to many resource allocation problems to find the solution in a distributed fashion. For example, this method is employed in [33] to solve the network utility maximization problem. The authors present the synchronous and asynchronous versions of GPA. The synchronous version of GPA is also used in [7], [34] to control charge powers of EVs in a power distribution system. In these papers the power grid is used as a medium for sending implicit messages from the end nodes to distributed controllers, thereby reducing the communication overhead. Although GPA exhibits stable convergence, its rate of convergence is linear, taking many iterations to converge especially in large distribution systems.

The second-order gradient-projection algorithm converges faster than the first-order algorithm. The scaled gradient-projection algorithm was discussed by Bertsekas and Tsitsiklis [35]. Our method differs from this method in two ways. First, they discuss the convergence of this algorithm under a different coordinate system (projection which is not vertically decomposable), whereas our method works for positive orthant projection. Second, we present sufficient conditions for the second-order projection method to converge super-linearly (or quadratically).

III. System Model

This work focuses on controlling residential EV chargers connected to the low-voltage feeders of a power distribution network, which has a tree-like (radial) operational structure at any given time and delivers power to various types of loads as shown in Figure 1. The root of this tree is the substation transformer which steps down the voltage from the transmission level to the primary distribution level. The leaf nodes in this tree (i.e., the end nodes) are loads connected to secondary distribution feeders. The intermediate nodes (i.e., Nodes $2-33$ in Figure 1) are the load buses in the primary distribution network. We assume that these nodes are connected to the secondary feeders via distribution transformers which step down the voltage to the secondary distribution level. Figure 1 shows a lateral originating from Node 25 in the primary network feeding several loads (homes, PEV chargers, etc.) connected to the secondary distribution network that spans a residential neighbourhood. The laterals originating from other nodes in the primary network and their downstream loads are not shown in this figure for brevity. We note that a leaf node in the secondary distribution network represents one or multiple homes (and the installed EV chargers). We assume that a leaf node has at least one upstream distribution transformer besides the substation transformer.

We aim to schedule EV charging to avoid overloading of transformers[1]. Following [7] we define the congestion state of a transformer as the difference between its rated capacity

[1]Equipment overloading in the distribution network is analogous to congestion in the Internet. Thus, we use transformer and link interchangeably throughout this paper.

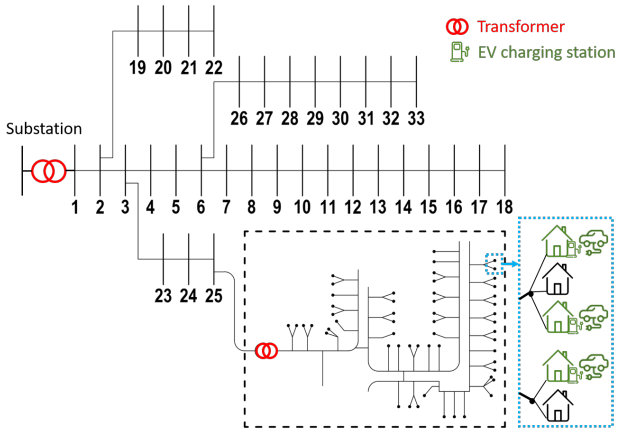

Fig. 1: The one-line diagram of a radial distribution network. The network is divided into primary (Nodes 1-33) and secondary feeders (an example shown in the dashed-box).

and its present loading level (both expressed in volt-ampere). We assume that a distribution-level phasor measurement unit (DPMU) is installed on the secondary-side of each transformer sampling the current passing through the transformer and its secondary voltage at short intervals (every few cycles for example). These phasor measurements can be easily converted to the apparent power loading of equipment. We also assume that there is point-to-point communication between EV chargers and the (distribution or substation) transformers that supply their demand. Figure 2 presents the logical view of the system with the communication links depicted by dotted lines. Similar to homes, the EV chargers located at the leaves of this network are supplied by the substation and (at least) one distribution transformer.

Each EV is characterized by a tuple $\langle U_e, \alpha_e, d_e, \sigma_e \rangle$ where $U_e(x_e)$ represents the utility of its owner (a measure of their satisfaction) which is an increasing function of its charge power x_e at any time, α_e represents its arrival time, d_e represents its energy demand (the difference between its current state-of-charge and its desired state-of-charge), and σ_e which is the user-specified deadline (the latest time by which its energy demand must be met). We denote the remaining charging duration by $\widetilde{\sigma}_e = \sigma_e - \alpha_e$. The specified deadline of an EV may not be precise, meaning that it may depart before or after its specified deadline. We use a discrete time model and assume that EVs arrive or depart at the beginning of a time slot. We denote the length of time slots by τ.

We denote the set of transformers installed in the distribution network by $\mathcal{L}$, the set of all connected EVs in the network by $\mathcal{E}$. We use matrix T to encode the point of connection of EV charging stations. In particular, $T_{el} = 1$ for every transformer l which supplies the charging station indexed by e. This element of the matrix is zero otherwise. Figure 2 shows an EV connected to a charging station e. This EV is supplied by distribution transformer l but not distribution transformer l'. Hence we have $T_{el} = 1$ and $T_{el'} = 0$. We denote the available

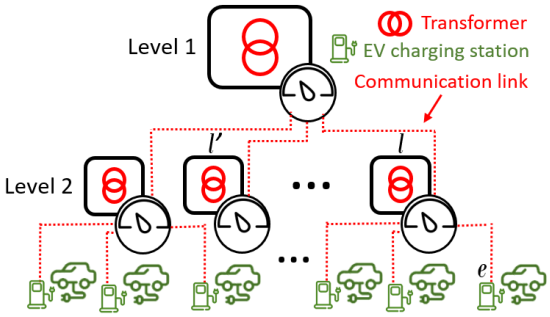

Fig. 2: The logical view of a radial distribution network.

capacity (i.e., the difference between its rated capacity and the total demand of inelastic loads downstream of the transformer) of transformer l by a_l. Note that we use a ballpark estimate of losses in primary and secondary distribution feeders and use a fixed power factor to calculate the loading of a transformer from the net demand of its downstream inelastic loads. This approximation leads to a small error as we discuss later.

We assume that each charging station keeps track of discrepancies between the claimed and true deadlines of the corresponding EV. Each time an EV is plugged in, the charging station records the specified deadline which is then compared with the time that the EV is unplugged from the charger. The charging station computes the difference between these two values, which we refer to as *historical discrepancy*, and stores it for every user (EV driver). The historical discrepancies collected in a fixed-size window are used by the charging station to update the reputation of a user at the beginning of each time slot. This reputation is used as a weight in the optimization problem discussed in the next section. In case of the centralized method, user reputation is sent to the central controller which solve the optimization problem. For decentralized methods, the reputation is used by the charging station to independently compute its charge power for the next time slot in a number of iterations.

The charging station is assumed to be tamper-resistant and can charge one EV at a time. It delays charging of an EV for some time, i.e., known as the *idle time*, if it is unplugged and plugged again after a short period of time. This prevents users from reporting an unrealistically early deadline and simulating a departure event at that deadline to maintain a high reputation.

IV. Methodology

A possible approach to charging EVs with different urgency parameters is to design a mechanism that allows EV drivers to buy electricity at a higher price if their charging demand is more urgent. This approach assumes the existence of a billing system and is therefore impractical in today's distribution grids, because existing electric vehicle supply equipment (EVSE) installed in residential buildings has a simple plug-and-charge interface. An alternative approach, which we take in this paper, is to design a real-time scheduling mechanism that relies on user-specified deadlines. These deadlines are modified according to the reputation of EV drivers, where the reputation is a numerical value calculated based on historical discrepancies as explained in this section.

A. Centralized Control of EV Charging Stations

In the beginning of a time slot, t, each active charging station computes a weight, $w_e(t) = f(\Delta_e, \Lambda_e(t))$ for the corresponding EV, where Δ_e is a statistic of historical discrepancies (e.g., the mean) and $\Lambda_e(t)$ is the laxity defined as

$$\Lambda_e(t) = \widetilde{\sigma}_e(t) - \frac{d_e(t)}{M_e}$$

where M_e is the maximum charge power supported by EVSE. The function f should have some intuitive properties. Specifically, it should be (a) positive valued and bounded (otherwise the objective function (2) may lose concavity); (b) decreasing as discrepancy or laxity becomes larger; (c) robust to outliers (i.e., outliers in historical data should not greatly affect the weight); (d) numerically stable, i.e., does not return very small or large values. Hence, we choose the following function that satisfies all these properties:

$$F(\Delta_e, \Lambda_e) = exp\left(\frac{-(\Delta_e + \Lambda_e)}{\beta}\right) \tag{1}$$

Here β is a scaling factor to normalize the sum, $\Delta_e + \Lambda_e$.

Let $0 < \zeta \leq 1$ be an efficiency factor that approximates losses in the distribution network. Hence, the effective capacity of transformer l can be written as ζa_l. Solving the following optimization problem yields the charge power, $x_e(t)$, of every charger e for interval $[t, t+1)$:

$$\text{maximize:} \quad \sum_{e \in E} w_e \log U_e(x_e) \tag{2}$$

$$\text{subject to:} \quad \sum_{e \in E} T_{el} x_e \leq \zeta a_l, \qquad \forall l \in \mathcal{L} \tag{3}$$

$$0 \leq x_e \leq M_e, \qquad \forall e \in \mathcal{E} \tag{4}$$

Suppose $U_e(x_e) = x_e$ and $w_e = F(\Delta_e, \Lambda_e)$. For brevity the time index is dropped from all variables in the above problem. This convex optimization problem can be modelled in CVXPY and solved using Mosek software. It is shown in [7] that the solution of this problem is a *proportionally fair* allocation of the available network capacity to EV chargers. We refer to this solution as the centralized solution and use it as a baseline.

B. Dual Problem and Projected Gradient Descent Algorithm

The Lagrangian function of the primal problem is:

$$g(\lambda) = \max_{0 \preceq x \preceq \mathcal{M}} \left\{ \sum_e w_e \log x_e + \sum_l \lambda_l \left(\zeta a_l - \sum_e T_{el} x_e \right) \right\}$$

where, $\lambda = (\lambda_1, \lambda_2, \ldots, \lambda_{|\mathcal{L}|}) \succeq 0$ are the Lagrangian multipliers for the constraints (3) and (4), respectively. Following [7], the Lagrangian function, $g(.)$ can be expressed more compactly as:

$$g(\lambda) = \sum_l \lambda_l \zeta a_l + \max_{0 \preceq x \preceq M} \left\{ \sum_e f_e(x_e; \lambda_e) \right\} \tag{5}$$

where

$$f_e(x_e;\lambda) = w_e \log x_e - \left(\sum_l \lambda_l T_{el}\right) x_e \tag{6}$$

Thus, the dual problem can be written as:

$$\begin{aligned} &\text{minimize: } g(\lambda) \\ &\text{subject to: } \lambda \succeq 0 \end{aligned} \tag{7}$$

By decomposing the dual problem into a number of subproblems that can be solved given the Lagrangian multipliers [36], it is possible to develop an iterative algorithm to compute the fair shares of EV chargers in a decentralized fashion. It requires synchronization among charging stations and sensors installed at transformers. This GPA-based method is described in Section IV-D and is considered as a baseline in this paper. In the next section, we propose a synchronous algorithm that is faster and has lower communication overhead compared to baseline algorithms.

C. Scaled Gradient Projection Algorithm (SGPA)

We propose a projected Newton's method that computes the second-order partial derivatives of the dual objective function. Specifically, in each iteration, it updates the Lagrange multiplier λ as follows:

$$\lambda^{(k+1)} = \left[\lambda^{(k)} - \gamma \left[D\left(\lambda^{(k)}\right)\right]^{-1} \nabla g\left(\lambda^{(k)}\right)\right]^{+} \tag{8}$$

Here k denotes a specific iteration, $0 < \gamma \leq 1$ is the step-size parameter, $\nabla g(.)$ is the gradient, and $D(.)$ is a diagonal matrix consisting of the principal-diagonal elements of the Hessian matrix H projected onto the positive axis:

$$[D(\lambda)]_{ll} = \begin{cases} \eta, & \text{if, } [H(\lambda)]_{ll} < \eta \\ [H(\lambda)]_{ll}, & \text{otherwise} \end{cases} \tag{9}$$

Note that η is a small positive number used to make the matrix D invertible, and

$$\begin{aligned} [H(\lambda)]_{ll} &= \frac{\partial^2 g}{\partial \lambda_l \partial \lambda_l} \\ &= \frac{\partial}{\partial \lambda_l}\left(\zeta a_l - \sum_e T_{el} x_e^*\right) \\ &= -\sum_e T_{el} \frac{\partial x_e^*}{\partial \lambda_l} \\ &\approx \left|\frac{\sum_e T_{el} \Delta x_e^*}{\Delta \lambda_l}\right| \\ &= \left|\frac{\text{load}_l^{(k)} - \text{load}_l^{(k-1)}}{\lambda_l^{(k)} - \lambda_l^{(k-1)}}\right| \end{aligned} \tag{10}$$

The last derivation above holds if inelastic demands change at a slower rate than the rate at which we update the charge power of EV chargers. Note that $[H(\lambda)]_{ll}$ is a non-negative number (cf. Eq. (20) in the appendix). Thus, we take the absolute value in the above derivations.

This algorithm exhibits some desirable properties: (a) *fast convergence*: in Theorem A.1 we show that, under some mild conditions, our algorithm converges super-linearly to the optimum point, which is an improvement over first-order projected gradient methods [7]; (b) *low computational cost*: computing the inverse of a diagonal matrix is easier than the inverse of Hessian and greatly reduces the computational cost of the Newton's method; (c) *low communication overhead*: this algorithm leverages only local information to compute the second-order partial derivatives; in Equation 10, each sensing node (installed at a transformer) only requires to track the previous loading level and λ.

Our decentralized EV charging algorithm is based on SGPA. Hence, it updates each Lagrangian multiplier and send this *congestion signal* to downstream charging stations. Algorithm 1, which is run at each sensing node (corresponding to a transformer) in the distribution network, describes the update that happens once in every iteration.

Algorithm 1: Algorithm for Transformer l

input : rating and measured load of transformer l
output: $\{\lambda_l^{(k+1)}\}$ which will be sent to downstream EV chargers

1 $\frac{\partial g}{\partial \lambda_l} \approx \text{rating}_l - \text{load}_l$
2 $\frac{\partial^2 g}{\partial \lambda_l^2} \approx \frac{\Delta load}{\Delta \lambda_l}$
3 $\lambda_l^{(k+1)} = \max\left\{\lambda_l^{(k)} - \gamma\left(\frac{\partial^2 g}{\partial \lambda_l^2}\right)^{-1} \frac{\partial g}{\partial \lambda_l}, 0\right\}$

When a charging station receives the Lagrangian multipliers from the substation and the distribution transformer supplying its demand, it computes its charge power:

$$x_e^{(k+1)} = \min\left\{\max\left\{\frac{w_e}{\sum_l T_{el}\lambda_l^{(k)}}, 0\right\}, M_e\right\} \tag{11}$$

and begins charging the connected EV with a power that equals $x_e^{(k+1)}$. Algorithm 2 updates the charge power of each EV.

Algorithm 2: Algorithm for EV charging station e

input : w_e and a sequence of $\{\lambda_l^{(k)}\}$ received from transformers supplying e ($l : T_{el} = 1$).
output: the charge power of charger e: $x_e^{(k+1)}$

1 $x_e^{(k+1)} = \min\left\{\max\left\{\frac{w_e}{\sum_{l:T_{el}=1}\lambda_l^{(k)}}, 0\right\}, M_e\right\}$

The change in the charge power of charging stations affects the loading of transformers, thereby enabling them to update the Lagrangian multiplier in every iteration. We assume that τ iterations take place in one time slot, i.e., in $[t, t+1)$, and the time between two consecutive iterations is on the order of hundred milliseconds.

D. Baseline Algorithms

To evaluate our proposed scaled gradient projection algorithm, we consider the following baseline algorithms:

Gradient Projection Algorithm (GPA): this is the decentralized algorithm outlined in Section IV-B. It is basically updating the Lagrangian multiplier using the projected gradient descent algorithm:

$$\lambda_l^{(k+1)} = \left[\lambda_l^{(k)} - \gamma \frac{\partial g}{\partial \lambda_l}\right]^+ \tag{12}$$

The gradient $\frac{\partial g}{\partial \lambda_l} = \zeta a_l - \sum_e T_{el} x_e^*$ can be calculated by simply subtracting the transformer loading (including the demands of elastic and inelastic loads) from its rated capacity as shown in [7]. Thus, we do not need to separately measure the demand of each EV charger.

Earliest Deadline First (EDF): it simply priorities charging EVs based on their deadlines; thus, EVs with earliest deadline are charged at the maximum rate supported by their charging station first. To fully utilize the network, we charge as many EVs as possible at any given time without overloading the transformers.

Least Laxity First (LLF): it is similar to EDF except that charging EVs is prioritized based on their laxity. EVs with the lowest laxity are charged at the maximum rate supported by the charging station first. At any point int time, we charge as many EVs as possible until the network is congested.

V. Case Studies

We implement the proposed EV charging mechanism and baselines introduced in Section IV-D in Python and use the simulation platform depicted in Figure 3 to compare their performance in four different simulation scenarios. The platform takes as input the structure of the distribution network, including points of connection of homes and EV charging stations, the household demands, the EV arrival and departure times, and the initial state-of-charge (SoC) of their batteries. To build the household demands, we take advantage of the real and reactive power consumption of several real homes. We use this data along with the charge powers of EVs determined by the algorithm to perform power flow analysis and obtain the loading levels of transformers. The sensor emulator module subsequently adds Gaussian noise to these values to imitate the measurement noise of sensors in real-world applications. These measurements are used to construct the congestion signal which is then sent to downstream EV charging stations via communication links. These signals are used by the control algorithm to update the charge power of EV charging stations in a single iteration.

The control algorithm needs to know which EVs will be connected to chargers in the next time step along with their demands and claimed deadlines. This data is produced by the traffic generator. We also store historical data about EVs to update their reputation throughout the simulation. Besides this data, the simulation platform adopts a battery model which expresses the capacity, and charge and discharge inefficiencies of the battery. This model is necessary to update the state-of-charge of the battery given its charge power.

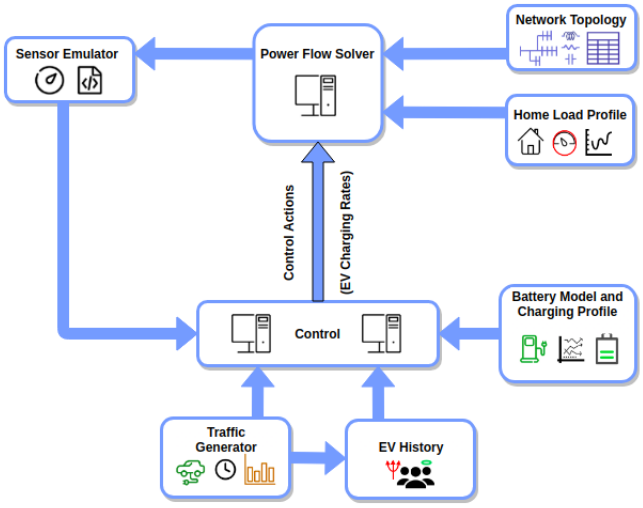

Fig. 3: Overview of the simulation framework.

A. Test System

We consider the 33-bus test system [37] shown in Figure 1 as the primary distribution network in our simulations. For modelling the secondary (low-voltage) distribution network, we assume that a feeder originates from every bus in the primary network (except Node 1). We adopt the IEEE European test feeder [38] as the secondary feeder. Figure 1 illustrates how a low-voltage network is connected to Node 25. We assume that a sensor, e.g., a distribution-level phasor measurement unit, is deployed at each of the transformer locations measuring the active and reactive powers in real time, and that there are communication links connecting the sensor at the substation to the sensors at distribution transformer locations, and these sensors to downstream charging stations.

There are 55 single-phase load connection points in each secondary feeder. Therefore, we have a total of 1760 (32×55) load connection points in the system. We assume a certain number of homes are connected to these points. To represent the household demand, we utilize sample household consumption data provided in the ADRES-CONCEPT project [39][2]. The data set contains real and reactive power consumption of 30 households with 1-second resolution over two weeks. Since our simulation spans one day, we split the data into 1-day segments. This yields 420 daily load profiles. We add white Gaussian noise with 10% standard deviation to each sample to increase the size of the data set; this way we create a total of 8400 unique household load data. We consider the active power consumption at the primary nodes provided in [37] to determine the appropriate level of aggregation at each low-voltage node (i.e., the houses connected to the same low-voltage node). We select houses randomly and connect them to a secondary node (i.e., a single-phase load connection point)

[2]The data was generated in the research project "ADRES-Concept" (EZ-IF: Development of concepts for ADRES- Autonomous Decentralized Regenerative Energy Systems, project no. 815 674). This project was funded by the Austrian Climate and Energy Fund and performed under the program "ENERGIE DER ZUKUNFT".

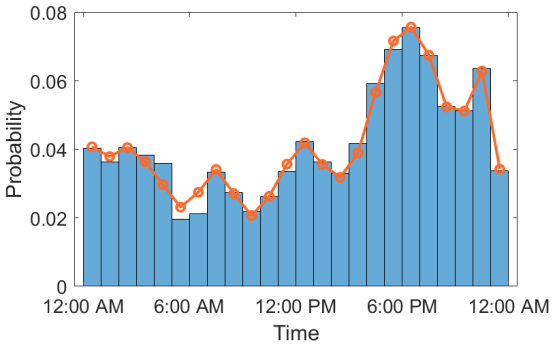

Fig. 4: Distribution of arrival times.

until the sum of all loads in the low-voltage network under each primary node matches the load given in the specification of the 33-bus system.

To have a realistic EV schedule (i.e., arrival and departure times of the EVs), we exploit the EV usage data provided in the Pecan Street data set [40]. The data set contains the power usage of many home appliances with up to 1-second resolution. We use the data recorded in 2016. Since there are only about 80 EVs in this data set, we take the daily arrival times of these EVs over one year and fit a Gaussian Mixture Model (GMM) to the probability distribution function (pdf). The distribution of arrival times and the fitted model with 7 Gaussian distributions are shown in Figure 4.

We assume that there are 500 EV chargers installed at random locations in our secondary distribution network. We sample the daily arrival times of the EVs from the fitted GMM. Since the Pecan Street data set does not provide the EV departure/disconnection times, we randomly sample the stay time of each EV from a Gaussian distribution with $\mu = 8$ and $\sigma = 2$ (in hours). The departure time is the sum of the arrival time and the stay time. The initial SoC of each EV when it arrives is sampled uniformly between 0 and 0.1. We consider 4 different battery sizes that belong to popular EVs in the market: a) $16kWh$ for Chevy Volt and Mitsubishi iMiEV, b) $30kWh$ for Nissan Leaf, c) $42kWh$ for BMW i3, and d) $75kWh$ for Tesla 3. For an EV, the battery size is selected randomly from the above types. We set the maximum charging rate to $\bar{M}_e = 7kW$ for all charging stations.

For SGPA and GPA, we define the step-size to be $\gamma = 0.008$ and 0.0008, respectively. We tune these values based on simulations, using the bounds suggested by our theoretical results as a hint. Furthermore, we assume 100 iterations in each time slot, which is 10 minutes long. Hence, the time between two iterations is 6 seconds.

B. Performance Metrics

Jain index: is used to evaluate fairness of a power allocation scheme (a higher value suggests a fairer scheme):

$$J(x) = \frac{(\sum_i x_i)^2}{n \sum_i x_i^2}$$

where x is a vector containing charge powers of all chargers in a given time slot and n is the number of active chargers.

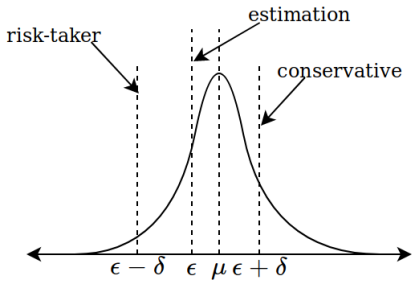

Fig. 5: Predicting and adjusting deadlines. μ and ϵ represent the actual and predicted deadlines respectively. Conservative (risk-taking) users add (subtract) δ to (from) their prediction.

Note that the Jain index is calculated for every time slot and then averaged over all time slots in one day.

Percentage of EVs with a certain SoC: it is the percentage of connected EVs with a SoC greater than or equal a certain threshold when they depart. We consider 90% as the threshold for Scenarios A, C and D (described below). For Scenario B, it is 80%.

Energy supplied above the rated capacity: it is the total amount of energy (in kWh) supplied by a transformer above its rated capacity for all the time slots in one day.

C. User Types

To study the efficacy of our charging mechanism, we consider conservative and risk-taking users. Both types estimate their duration of stay based on their information, but report their estimation after a slight modification. This modification is necessary as they may not know precisely when their EV will be used again. In particular, *conservative* users add a positive offset to their estimation so that they reduce the chance of declaring a deadline before their actual deadline when their estimation is not precise. This helps this type of users to maintain a better reputation in the system. Unlike conservative users, *risk-taking* users subtract a non-negative offset from their estimation, running the risk of ruining their reputation if the actual deadline is after their declared deadline.

Figure 5 presents the difference between these user types. We consider historical discrepancy data for the past 3 days and take their average to compute Δ_e. To obtain each discrepancy, we have to model how EV drivers predict their deadline. We sample their prediction from a Gaussian distribution which has the same mean as the true deadline and $\sigma = 0.5$. To simulate conservative (risk-taking) users, we add (subtract) a positive number, δ, to (from) the predicted deadline, where δ is sampled from a Gaussian distribution with $\mu = 3$ and $\sigma = 0.5$ (in hours). This gives us the user-specified deadline.

Based on these two user types, we develop four scenarios: (a) *Scenario A*: both types of EV drivers are present in the system (50% of population each) and all the other parameters (arrival times and locations) are sampled as described earlier, (b) *Scenario B*: is similar to Scenario A except that the arrival times and connection points of EVs are chosen in such a way that the first transformer is congested, (c) *Scenario C*: only conservative users are in the system, and (d) *Scenario D*: only

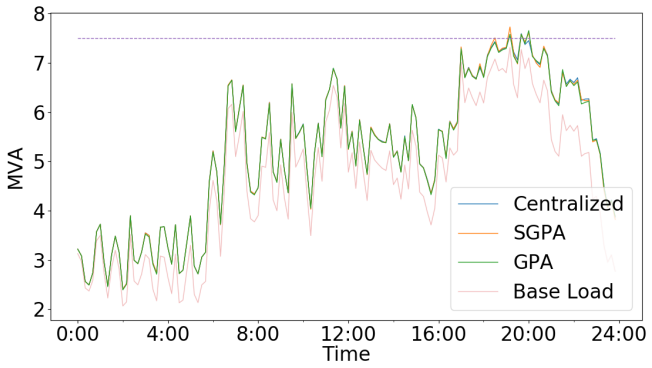

Fig. 6: Substation loading at different time slots for centralized, GPA and SGPA. The horizontal (purple) dashed line represents the rating of the substation transformer.

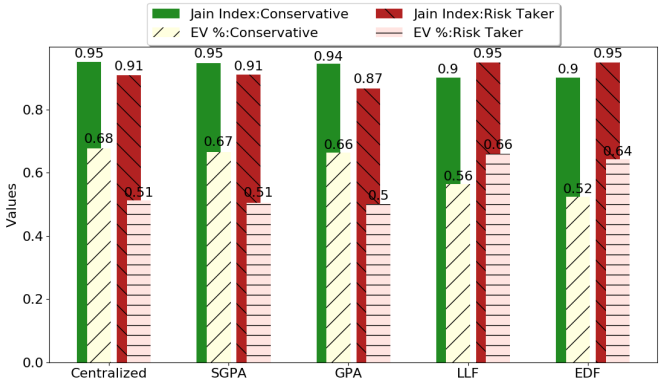

Fig. 7: Comparing performance of different algorithms for conservative and risk-taking users (Scenario A).

risk-taking users are in the system. In the first two scenarios, we assume that risk-taking users have lower reputation compared to the conservative users when the simulation starts.

D. Scenario A

Figure 6 shows the substation transformer's loading for centralized, GPA, SGPA, and baseline algorithms. The congestion period is from 6:00pm to 9:00pm. It can be readily seen that, for most of the time, GPA and SGPA follow the centralized solution. Note that LLF and EDF policies are quite similar to the centralized solution so we do not show them in this figure.

Figure 7 compares the performance of different algorithms considering the first two performance metrics presented in Section V-B. The centralized algorithm outperforms least-laxity-first and earliest-deadline-first both in terms of fairness and percentage of EVs with $\geq 90\%$ SoC for both conservative and risk-taking users. Moreover, the performance gap between two types of users for the centralized algorithm is higher than baseline algorithms. This indicates that our centralized mechanism can better differentiate between the two types of users than baseline algorithms. Both of the distributed algorithms follow the power allocation of the centralized algorithm most of the time. That said, our mechanism (SGPA) follows the centralized solution more closely than GPA. We attribute this to the faster convergence of this algorithm.

E. Scenario B

To investigate the performance of our proposed methods during congestion, we study a scenario in which 54 EVs (27 conservative and 27 risk-taking) arrive at same time (i.e., 9:00am) to charging stations that are fed by the same distribution transformer (i.e., the first distribution transformer). The initial SoC (5%) and claimed charging duration (8 hours) are the same for all EVs. This ensures that the distribution transformer is congested for a relatively long period of time. However, conservative and risk-taking users stay in the system for 7 and 9 hours, respectively (hence, the discrepancy is 1 hour). Figure 8 and 9 depict the transformer loading for different algorithms during the congestion period. Both SGPA

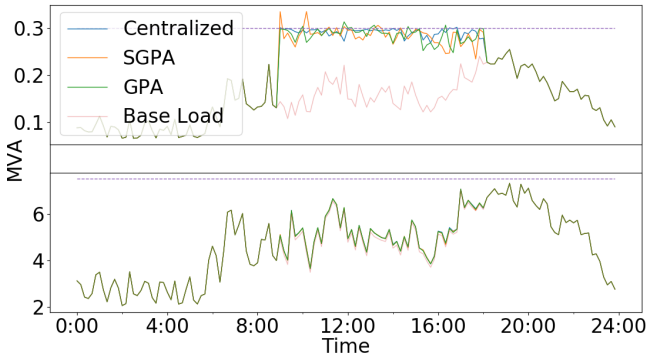

Fig. 8: Transformer loading over one day using centralized, SGPA and GPA. The top plot is for a distribution transformer and the bottom one is for the substation transformer.

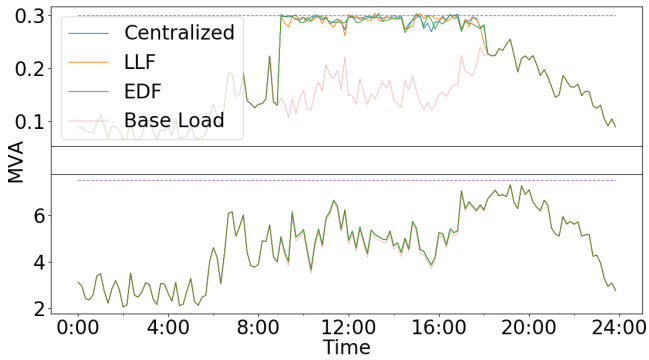

Fig. 9: Transformer loading over one day using centralized, LLF and EDF. The top plot is for a distribution transformer and the bottom one is for the substation transformer.

and GPA (as well as LLF and EDF) follow the centralized algorithm, though they exhibit some fluctuations.

Figure 10 shows the performance of all the algorithms in this scenario. The centralized algorithm, just as SGPA and GPA, assigns a higher priority to conservative users because of their better reputation. In fact for the centralized algorithm, all the EVs are charged up to 80% of their capacity by the end of the simulation. However, LLF and EDF algorithms provide more power to risk-taking users than our proposed algorithms

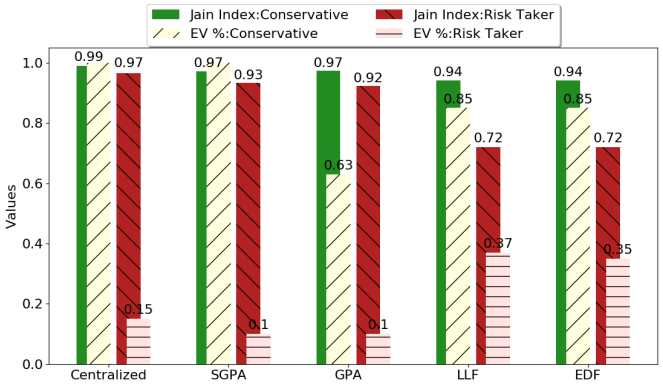

Fig. 10: Comparing performance of different algorithms for conservative and risk-taking users (Scenario B).

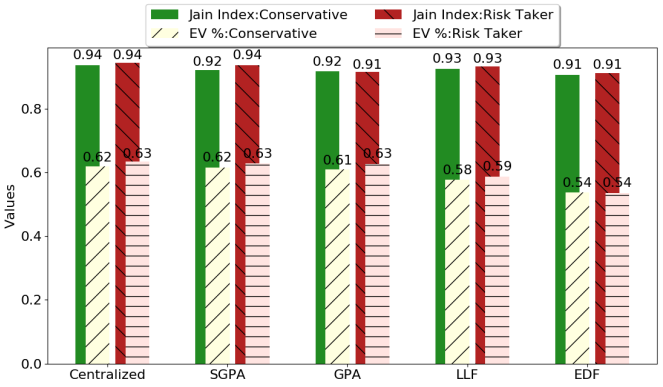

Fig. 11: Comparing performance of different algorithms for conservative and risk-taking users (Scenarios C and D).

as they neglect their reputation.

F. Scenario C & D

Figure 11 compares the performance of different algorithms in Scenarios C and D, which consist of only conservative and risk-taking users, respectively. As expected, when all the users belong to the same category, our mechanism does not differentiate between them. Here, the difference in performance between the two types is merely due to the different laxity values they have.

G. Analyzing the Rate of Convergence

Figure 12 compares the rate of convergence of SGPA and GPA. This analysis is done for a time slot (7:00pm) in Scenario A when the network is congested. Here, convergence is defined as the event when the total power allocated by SGPA (or by GPA) reaches 95% of the total power allocated by the centralized algorithm. As the step-size becomes larger, GPA converges in fewer iterations. Interestingly, SGPA converges after less than 8 iterations, irrespective of the step size.

H. Excursion from the Rated Capacity

When the network is congested, SGPA and GPA may overshoot the target, thereby loading the transformer above its rated capacity temporarily. Table I shows the total energy (in kWh) supplied above the rated capacity of the substation

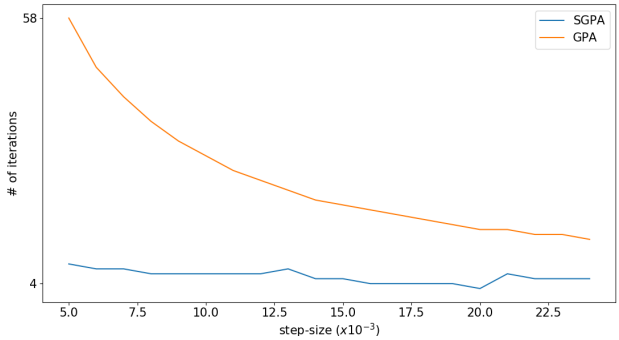

Fig. 12: 95% convergence analysis of SGPA and GPA for a specific time slot (7:00 pm) for scenario A. Here the initial points for both algorithms are same

TABLE I: Energy supplied above the rated capacity of a transformer. In Scenarios A, C and D, the values are calculated for the substation; In Scenario B, it is computed for the first distribution transformer.

	Energy supplied above the rated capacity	
	SGPA	GPA
Scenario A	70.58 kWh	52.81 kWh
Scenario B	5.78 kWh	2.28 kWh
Scenario C	58.50 kWh	46.96 kWh
Scenario D	93.51 kWh	48.14 kWh

transformer by centralized, SGPA and GPA for Scenarios A, C and D. For Scenario B, we examine the first distribution transformer which is expected to be overloaded. As expected, both SGPA and GPA overload the transformer for a short period of time; SGPA results in slightly higher overloading which we attribute to its higher responsiveness. In any case, this level of overloading is not problematic because transformers can be loaded above their rated capacity for a short period of time without being excessively overheated.

VI. Conclusions and Future Work

This paper presents a deadline-aware, reputation-based, proportionally fair and efficient power allocation to EV charging stations connected to a power distribution network. This power allocation is determined in real time by individual charging stations using a decentralized algorithm which converges rapidly to the available capacity of the network. The proposed algorithm has a lower communication overhead as it utilizes the power system instead of sending explicit messages from charging stations to nodes installed in the network. Hence the only communication that is necessary is for sending congestion signals to the charging stations. We show through extensive simulations that our algorithm tracks the available capacity of the network, favors conservative users (with better reputation), and is as efficient as a centralized control algorithm. We also prove that the scaled gradient projection algorithm has quadratic convergence under some conditions.

Our work has several limitations that we plan to address in the future. Specifically, we assume that the hessian matrix of the dual objective function is almost diagonal at the optimum point in Theorem A.1. We have not verified whether this assumption holds in practice; nevertheless, our simulations

have so far shown the superior rate of convergence over the first-order gradient projection algorithm. We intend to perform extensive experiments with data obtained from a real test system to further corroborate our theoretical results in future work. Furthermore, the weight function defined in Section IV-A can have other forms. The design of an incentive compatible mechanism is deferred to future work. Lastly, we use the DC approximation of power flow in distribution systems and therefore cannot address voltage problems that may occur as a result of charging a large number of EVs.

REFERENCES

[1] L. C. Casals *et al.*, "Sustainability analysis of the electric vehicle use in europe for CO2 emissions reduction," *Journal of Cleaner Production*, vol. 127, pp. 425–437, 2016.

[2] J. A. P. Lopes, F. J. Soares, and P. M. R. Almeida, "Integration of electric vehicles in the electric power system," *Proceedings of the IEEE*, vol. 99, no. 1, pp. 168–183, 2011.

[3] M. Yilmaz and P. T. Krein, "Review of the impact of vehicle-to-grid technologies on distribution systems and utility interfaces," *IEEE Transactions on power electronics*, vol. 28, no. 12, pp. 5673–5689, 2013.

[4] S. Chen, Y. Ji, and L. Tong, "Deadline scheduling for large scale charging of electric vehicles with renewable energy," in *2012 IEEE 7th Sensor Array and Multichannel Signal Processing Workshop (SAM)*. IEEE, 2012, pp. 13–16.

[5] E. Sortomme *et al.*, "Coordinated charging of plug-in hybrid electric vehicles to minimize distribution system losses," *IEEE transactions on smart grid*, vol. 2, no. 1, pp. 198–205, 2011.

[6] R. Mehta *et al.*, "Smart charging strategies for optimal integration of plug-in electric vehicles within existing distribution system infrastructure," *IEEE Transactions on Smart Grid*, vol. 9, no. 1, pp. 299–312, 2018.

[7] O. Ardakanian, C. Rosenberg, and S. Keshav, "Distributed control of electric vehicle charging," in *Proceedings of the fourth international conference on Future energy systems*. ACM, 2013, pp. 101–112.

[8] C. Ahn, C.-T. Li, and H. Peng, "Optimal decentralized charging control algorithm for electrified vehicles connected to smart grid," *Journal of Power Sources*, vol. 196, no. 23, pp. 10 369–10 379, 2011.

[9] M. C. Kisacikoglu, F. Erden, and N. Erdogan, "Distributed control of pev charging based on energy demand forecast," *IEEE Transactions on Industrial Informatics*, vol. 14, no. 1, pp. 332–341, 2018.

[10] Y. Cao *et al.*, "A decentralized deadline-driven electric vehicle charging recommendation," *IEEE Systems Journal*, no. 99, pp. 1–12, 2018.

[11] Z. Huang *et al.*, "Discovering valuations and enforcing truthfulness in a deadline-aware scheduler," in *IEEE Conference on Computer Communications (INFOCOM)*. IEEE, 2017.

[12] M. M. Nejad, L. Mashayekhy, and D. Grosu, "Truthful greedy mechanisms for dynamic virtual machine provisioning and allocation in clouds," *IEEE transactions on parallel and distributed systems*, vol. 26, no. 2, pp. 594–603, 2015.

[13] O. Ardakanian, *Advances in Distribution System Monitoring*. Springer International Publishing, 2018, pp. 1–3.

[14] M. Liu *et al.*, "Decentralized charging control of electric vehicles in residential distribution networks," *IEEE Transactions on Control Systems Technology*, vol. 27, no. 1, pp. 266–281, 2019.

[15] J. Quirós-Tortós *et al.*, "Control of EV charging points for thermal and voltage management of LV networks," *IEEE Transactions on Power Systems*, vol. 31, no. 4, pp. 3028–3039, 2016.

[16] K. Kaur, M. Singh, and Kumar, "Multiobjective optimization for frequency support using electric vehicles: An aggregator-based hierarchical control mechanism," *IEEE Systems Journal*, vol. 13, no. 1, pp. 771–782, 2019.

[17] K. Kaur *et al.*, "A colored petri net based frequency support scheme using fleet of electric vehicles in smart grid environment," *IEEE Transactions on Power Systems*, vol. 31, no. 6, pp. 4638–4649, 2016.

[18] Z. Liu *et al.*, "Optimal day-ahead charging scheduling of electric vehicles through an aggregative game model," *IEEE Transactions on Smart Grid*, vol. 9, no. 5, pp. 5173–5184, 2018.

[19] J. Zhao *et al.*, "Risk-based day-ahead scheduling of electric vehicle aggregator using information gap decision theory," *IEEE Transactions on Smart Grid*, vol. 8, no. 4, pp. 1609–1618, 2017.

[20] K. Kaur, N. Kumar, and M. Singh, "Coordinated power control of electric vehicles for grid frequency support: MILP-based hierarchical control design," *IEEE Transactions on Smart Grid*, 2019.

[21] S. Bansal, M. N. Zeilinger, and C. J. Tomlin, "Plug-and-play model predictive control for electric vehicle charging and voltage control in smart grids," in *53rd IEEE Conference on Decision and Control*, 2014.

[22] X. Luo and K. W. Chan, "Real-time scheduling of electric vehicles charging in low-voltage residential distribution systems to minimize power losses and improve voltage profile," *IET Generation, Transmission, Distribution*, vol. 8, no. 3, pp. 516–529, 2014.

[23] J. Hu, S. You, M. Lind, and J. Ostergaard, "Coordinated charging of electric vehicles for congestion prevention in the distribution grid," *IEEE Transactions on Smart Grid*, vol. 5, no. 2, pp. 703–711, 2014.

[24] J. Rivera *et al.*, "Alternating direction method of multipliers for decentralized electric vehicle charging control," in *52nd IEEE Conference on Decision and Control*. IEEE, 2013, pp. 6960–6965.

[25] M. Liu, Y. Shi, and X. Liu, "Distributed MPC of aggregated heterogeneous thermostatically controlled loads in smart grid," *IEEE Transactions on Industrial Electronics*, vol. 63, no. 2, pp. 1120–1129, 2016.

[26] M. Liu, P. K. Phanivong, and D. S. Callaway, "Customer-and network-aware decentralized EV charging control," in *Power Systems Computation Conference (PSCC)*. IEEE, 2018, pp. 1–7.

[27] A. Alyousef and H. de Meer, "Design of a TCP-like smart charging controller for power quality in electrical distribution systems," in *10th International Conference on Future Energy Systems (e-Energy)*. ACM, 2019, pp. 128–138.

[28] J. Hong, X. Tan, and D. Towsley, "A performance analysis of minimum laxity and earliest deadline scheduling in a real-time system," *IEEE Transactions on Computers*, vol. 38, no. 12, pp. 1736–1744, 1989.

[29] P. Moyal, "On queues with impatience: stability, and the optimality of earliest deadline first," *Queueing Systems*, vol. 75, no. 2-4, pp. 211–242, 2013.

[30] K. Gardner, S. Borst, and M. Harchol-Balter, "Optimal scheduling for jobs with progressive deadlines," in *IEEE Conference on Computer Communications (INFOCOM)*. IEEE, 2015, pp. 1113–1121.

[31] Y. Nakahira, A. Ferragut, and A. Wierman, "Minimal-variance distributed deadline scheduling in a stationary environment," *ACM SIGMETRICS PER*, vol. 46, no. 3, pp. 56–61, 2019.

[32] Y. Nakahira *et al.*, "Smoothed least-laxity-first algorithm for EV charging," in *8th International Conference on Future Energy Systems (e-Energy)*. ACM, 2017, pp. 242–251.

[33] S. H. Low and D. E. Lapsley, "Optimization flow control. i. basic algorithm and convergence," *IEEE/ACM Transactions on networking*, vol. 7, no. 6, pp. 861–874, 1999.

[34] O. Ardakanian, S. Keshav, and C. Rosenberg, "Real-time distributed control for smart electric vehicle chargers: From a static to a dynamic study," *IEEE Transactions on Smart Grid*, vol. 5, no. 5, pp. 2295–2305, 2014.

[35] D. P. Bertsekas and J. N. Tsitsiklis, *Parallel and distributed computation: numerical methods*. Prentice hall Englewood Cliffs, NJ, 1989, vol. 23.

[36] D. P. Palomar and M. Chiang, "A tutorial on decomposition methods for network utility maximization," *IEEE Journal on Selected Areas in Communications*, vol. 24, no. 8, pp. 1439–1451, Aug 2006.

[37] M. E. Baran and F. F. Wu, "Network reconfiguration in distribution systems for loss reduction and load balancing," *IEEE Transactions on Power Delivery*, vol. 4, no. 2, pp. 1401–1407, 1989.

[38] IEEE PES distribution systems analysis subcommittee, radial test feeders. [Online]. Available: http://sites.ieee.org/pes-testfeeders/resources/

[39] ADRES dataset. https://www.ea.tuwien.ac.at/projects/adres_concept/EN/. [Online].

[40] Pecan Street dataset. https://dataport.pecanstreet.org/. [Online].

[41] R. M. Freund, "Newton's method for unconstrained optimization," 2004.

APPENDIX

A. Vector and Matrix Norms

Let x be a d dimensional vector, A be a symmetric $d \times d$ matrix, A' be its transpose and $\|.\|_k$ be a vector norm (or an induced norm for matrices). From Reference [35] we have these propositions:

1) $\|x\|_1 \leq \sqrt{d}\,\|x\|_2 \leq \sqrt{d}\,\|x\|_1$
2) $\|Ax\| \leq \|A\|\,\|x\|$
3) $\|AB\| \leq \|A\|\,\|B\|$ [Let B be a $d \times d$ matrix]
4) $\|A\|_1 \leq \sqrt{d}\,\|A\|_2$
5) $\|A\|_\infty = \|A'\|_1 = \|A\|_1$
6) $\|A\|_2^2 \leq \|A\|_\infty \|A\|_1$
7) $\|A\|_1 \leq \sqrt{d}\,\|A\|_2 \leq \sqrt{d}\,\|A\|_1$

Proposition 7 is derived from Propositions 4, 5, and 6.

B. Projections

In (9), we use a matrix projection which can be written as:

$$[A]^\eta = \arg\min_{D \in \mathcal{D}} \|A - D\|_2$$

where $\mathcal{D}$ is the set of diagonal matrices whose diagonal components are greater than or equal to a small positive number η. More precisely:

$$\mathcal{D} = \left\{ D \in \mathbb{R}^{d \times d} | D \text{ is diagonal and, } [D]_{ll} \geq \eta > 0, \forall l \right\}$$

It is easy to verify that $[A]^\eta$ is invertible, $[[A]^\eta]^{-1} \leq \frac{1}{\eta}$, and $\mathcal{D}$ is a nonempty and closed convex set. Hence, this projection is non-expansive [See [35], Page 211, Proposition 3.2.:(c)]:

$$\begin{aligned} \|[A]^\eta - [B]^\eta\|_2 \leq \|A - B\|_2 \implies \\ \sqrt{d}\,\|[A]^\eta - [B]^\eta\|_2 \leq \sqrt{d}\,\|A - B\|_2 \implies \\ \|[A]^\eta - [B]^\eta\|_1 \leq \sqrt{d}\,\|A - B\|_1 \end{aligned} \tag{13}$$

Similarly in (8), we use a projection that can be written as:

$$[\lambda]^+ = \arg\min_{\mu \in \mathcal{C}} \|\lambda - \mu\|_2$$

where $\mathcal{C} = \left\{ \mu | \mu \in \mathbb{R}^d, \mu \succeq 0 \right\}$. This projection is also non-expansive. Thus, we have:

$$\begin{aligned} \left\| [\lambda]^+ - [\mu]^+ \right\|_2 \leq \|\lambda - \mu\|_2 \implies \\ \left\| [\lambda]^+ - [\mu]^+ \right\|_1 \leq \sqrt{d}\,\|\lambda - \mu\|_1 \end{aligned} \tag{14}$$

C. Quadratic Convergence of SGPA

Theorem A.1. *Let $g(\lambda)$ be a twice continuously differentiable function in the domain $\mathcal{C} = \left\{ \lambda \in \mathbb{R}^d | \lambda \succeq 0 \right\}$, $\lambda^* \in \mathcal{C}$ be a point such that $\nabla g(\lambda^*) = 0$, $H(\lambda)$ be the Hessian matrix, $D(\lambda) = [H(\lambda)]^\eta$ be a diagonal matrix, and the following assumptions hold:*

(i) the Hessian matrix is diagonal and invertible at λ^*, i.e., $H(\lambda^*) = [H(\lambda^*)]^\eta$ for some small η;

(ii) there exist constants $L > 0$, $\theta > 0$ such that $\forall \lambda, \mu \in \mathcal{D}$ we have $\|H(\lambda) - H(\mu)\|_1 \leq L\,\|\lambda - \mu\|_1$ if $\|\lambda - \mu\|_1 \leq \theta$.

Now if $\lambda^{(k+1)} = \left[\lambda^{(k)} - \gamma D\left(\lambda^{(k)}\right)^{-1} \nabla g\left(\lambda^{(k)}\right)\right]^+$ and $\gamma \to 1$ then we have the following:

1) $\left\|\lambda^{(k+1)} - \lambda^*\right\|_1 \leq \frac{L}{\eta}\left(\frac{\gamma\sqrt{d}}{2} + d\right)\left\|\lambda^{(k)} - \lambda^*\right\|_1^2$

2) $\left\|\lambda^{(k+1)} - \lambda^*\right\| < \left\|\lambda^{(k)} - \lambda^*\right\|$, if $\left\|\lambda^{(k)} - \lambda^*\right\|_1 < \frac{\eta}{\left(\frac{\gamma\sqrt{d}}{2} + d\right)L}$

Proof. The proof idea is similar to [41]. For convenience we use the following notation: $\lambda := \lambda^{(k)}$, $H_t := H(\lambda^* + t(\lambda - \lambda^*))$, $H^* := H(\lambda^*)$, $D := D(\lambda)$, $D^* := D(\lambda^*)$, $\nabla g := \nabla g(\lambda)$ and $\nabla g^* := \nabla g(\lambda^*)$. Based on (14) and (13) we have the following derivation:

$$\begin{aligned} &\|\gamma H_t - D\|_1 = \|\gamma H_t - \gamma H^* + \gamma H^* - D\|_1 \\ &\leq \gamma\,\|H_t - H^*\|_1 + \|\gamma H^* - D\|_1 \\ &\leq \gamma\,\|H_t - H^*\|_1 + \|H^* - D\|_1 + (1 - \gamma)\,\|H^*\|_1 \\ &\approx \gamma\,\|H_t - H^*\|_1 + \|H^* - D\|_1 \qquad \text{as } \gamma \to 1 \\ &= \gamma\,\|H_t - H^*\|_1 + \|[H^*]^\eta - [H]^\eta\|_1 \\ &\leq \gamma\,\|H_t - H^*\|_1 + \sqrt{d}\,\|H^* - H\|_1 \\ &\leq \gamma L\,\|t(\lambda - \lambda^*)\|_1 + \sqrt{d}L\,\|\lambda - \lambda^*\|_1 \\ &= \left(\gamma t + \sqrt{d}\right) L.\,\|\lambda - \lambda^*\|_1 \end{aligned} \tag{15}$$

Let $\phi(t) = \nabla g\left(\lambda^* + t\left(\lambda - \lambda^*\right)\right)$. Then $\phi'(t) = H_t.(\lambda - \lambda^*)$ and

$$\nabla g - \nabla g^* = \phi(1) - \phi(0) = \int_0^1 H_t.(\lambda - \lambda^*)dt \tag{16}$$

Based on the propositions and equations, we have the following derivation:

$$\begin{aligned} &\left\|\lambda^{(k+1)} - \lambda^*\right\|_1 \leq \sqrt{d}\left\|\lambda^{(k+1)} - \lambda^*\right\|_2 \\ &= \sqrt{d}\left\|\lambda^{(k+1)} - [\lambda^*]^+\right\|_2 \qquad \text{since } [\lambda^*]^+ = \lambda^* \\ &= \sqrt{d}\left\|\left[\lambda - \gamma D^{-1}\nabla g\right]^+ - [\lambda^*]^+\right\|_2 \\ &\leq \sqrt{d}\left\|\lambda - \gamma D^{-1}\nabla g - \lambda^*\right\|_2 \\ &= \sqrt{d}\left\|\lambda - \lambda^* - \gamma D^{-1}\left(\nabla g - \nabla g^*\right)\right\|_2 \\ &= \sqrt{d}\left\|\lambda - \lambda^* - D^{-1}\int_0^1 \gamma H_t.(\lambda - \lambda^*)dt\right\|_2 \\ &= \sqrt{d}\left\|D^{-1}\left(\int_0^1 (\gamma H_t - D).(\lambda - \lambda^*)dt\right)\right\|_2 \\ &\leq \sqrt{d}\left\|D^{-1}\left(\int_0^1 (\gamma H_t - D).(\lambda - \lambda^*)dt\right)\right\|_1 \\ &\leq \sqrt{d}\left\|D^{-1}\right\|\int_0^1 \|\gamma H_t - D\|_1\,\|\lambda - \lambda^*\|_1\,dt \\ &= \sqrt{d}\left\|D^{-1}\right\|\|\lambda - \lambda^*\|_1\int_0^1 \|\gamma H_t - D\|_1\,dt \\ &\leq \sqrt{d}\left\|D^{-1}\right\|\|\lambda - \lambda^*\|_1\int_0^1 \left(\gamma t + \sqrt{d}\right) L.\,\|\lambda - \lambda^*\|_1\,dt \\ &= \sqrt{d}\left\|D^{-1}\right\|\|\lambda - \lambda^*\|_1^2\int_0^1 \left(\gamma t + \sqrt{d}\right) Ldt \\ &= \left\|D^{-1}\right\|\|\lambda - \lambda^*\|_1^2\left(\frac{\gamma\sqrt{d}}{2} + d\right) L \end{aligned}$$

$$\leq \left(\frac{\gamma\sqrt{d}}{2}+d\right)\frac{L}{\eta}\left\|\lambda-\lambda^*\right\|_1^2 \tag{17}$$

$$< \left\|\lambda-\lambda^*\right\|_1 \tag{18}$$

Note that (17) and (18) prove the first and second parts of the theorem, respectively. □

D. Values of d and L

Here d is the dimension of λ or equivalently the number of transformers in the system. As we use the IEEE 33-bus system, $d = 33$ in our test system. To find the value of L, we first list the following definitions and propositions:

$$g_k = \frac{\partial g}{\partial \lambda_k} = a_k - \sum_e T_{ek} x_e^* \tag{19}$$

$$g_{kl} = \frac{\partial^2 g}{\partial \lambda_k \partial \lambda_l} = -\sum_e T_{ek}\frac{\partial x_e^*}{\partial \lambda_l} = \sum_e T_{ek}T_{el}\frac{(x_e^*)^2}{w_e} \tag{20}$$

$$\nabla g_k = (g_{k1}, g_{k2}, \ldots, g_{kd}) \tag{21}$$

$$g_{kll'} = \frac{\partial^3 g}{\partial \lambda_k \partial \lambda_l \partial \lambda_l'} = -\sum_e T_{ek}T_{el}T_{el'}\frac{2(x_e^*)^3}{w_e^2} \tag{22}$$

$$M = \max_e\{M_e\} \qquad w = \min_e\{w_e\} \tag{23}$$

$$\widetilde{L} = \max_e \sum_{l'} T_{el'} \qquad \widetilde{E} = \max_l \sum_e T_{el} \tag{24}$$

Note that, the charge power, x_e (so the dual objective function, g) is not rigorously differentiable for all, $\lambda \succeq 0$. It is because of the projection we use on x_e (11) changes abruptly at $x_e = M_e$. We can approximate this sharp change by a smooth function. In that case, x_e and g will become differentiable at all points and (19), (20) and (22) will hold. Also from (11), g_{kl} and $g_{kll'}$ will be zero, if $\frac{w_e}{\sum_l T_{el}\lambda_l} > M_e$.

Now we show that ∇g_k is Lipschitz continuous (i.e. $\|\nabla g_k(\lambda) - \nabla g_k(\mu)\|_1 \leq L\|\lambda-\mu\|_1$) by showing that the corresponding Hessian, $[\mathcal{H}_k]_{ll'} = g_{kll'}$, is bounded, i.e., $\|\mathcal{H}_k\|_1 \leq L$:

$$\|\mathcal{H}_k\|_1 = \max_l \sum_{l'} |g_{kll'}| \leq \sum_e T_{ek}T_{el}T_{el'}\frac{2(x_e^*)^3}{w_e^2}$$

$$\leq \frac{2}{w^2}\sum_e T_{el}T_{el'}(x_e^*)^3 \qquad \text{since } T_{ek} \leq 1$$

$$\leq \frac{2M^3}{w^2}\max_l \sum_{l'}\sum_e T_{el}T_{el'}$$

$$\leq \frac{2M^3}{w^2}\max_l \sum_e T_{el}\widetilde{L} \leq \frac{2M^3}{w^2}\widetilde{L}\widetilde{E} \implies$$

$$\|\nabla g_k(\lambda) - \nabla g_k(\mu)\|_1 \leq \frac{2M^3}{w^2}\widetilde{L}\widetilde{E}\|\lambda-\mu\|_1 \tag{25}$$

We have

$$\|H(\lambda) - H(\mu)\|_1 = \max_m \sum_l |g_{lm}(\lambda) - g_{lm}(\mu)|$$

$$= \sum_l |g_{lk}(\lambda) - g_{lk}(\mu)| \qquad \text{let, } k \text{ be the argmax}$$

$$= \|\nabla g_k(\lambda) - \nabla g_k(\mu)\|_1$$

$$\leq \frac{2M^3}{w^2}\widetilde{L}\widetilde{E}\|\lambda-\mu\|_1$$

$$\implies L = \frac{2M^3}{w^2}\widetilde{L}\widetilde{E}$$

Hence in our test network, the parameters should be set as follows:

- $\gamma \to 1$
- $L = \frac{2M^3\widetilde{L}\widetilde{E}}{w^2}$
- $d = 33$

E. Proof of Descent Direction Update

The projection in (8) can be written as

$$\lambda^{(k+1)} = \lambda^{(k)} - \gamma S D^{-1}\nabla g$$

Here, S is a diagonal matrix defined as follows:

$$S_{ii} = \begin{cases} 1, & \text{if } \gamma[D^{-1}\nabla g]_i \leq \lambda_i^{(k)} \\ \frac{\lambda_i^{(k)}}{\gamma[D^{-1}\nabla g]_i}, & \text{if } \gamma[D^{-1}\nabla g]_i > \lambda_i^{(k)} \end{cases} \tag{26}$$

This matrix scales each component of the vector, $\gamma D^{-1}\nabla g$, to project the difference (i.e., $\lambda^{(k)} - \gamma D^{-1}\nabla g$) on the positive orthant. Since SD^{-1} is a non-negative diagonal matrix, the direction, $-\gamma SD^{-1}\nabla g$, is a descent direction.

F. Convergence Rate Analysis

Definition: We say that a sequence of real vectors $\{v_k\}$ converging to v^*, has a super-linear rate of convergence (under a vector norm, $\|.\|$) if

$$\lim_{k\to\infty}\frac{\|v_{k+1}-v^*\|}{\|v_k - v^*\|} = 0$$

From (18) it is evident that, near λ^*, the sequence, $\left\{\lambda^{(k)}\right\}$ converges to λ^* (i.e., $\lim_{k\to\infty}\left\|\lambda^{(k)}-\lambda^*\right\|_1 \to 0$). From (17) we have:

$$\frac{\left\|\lambda^{(k+1)}-\lambda^*\right\|_1}{\left\|\lambda^{(k)}-\lambda^*\right\|_1} \leq \left(\frac{\gamma\sqrt{d}}{2}+d\right)\frac{L}{\eta}\left\|\lambda^{(k)}-\lambda^*\right\|_1$$

$$\implies \lim_{k\to\infty}\frac{\left\|\lambda^{(k+1)}-\lambda^*\right\|_1}{\left\|\lambda^{(k)}-\lambda^*\right\|_1} = 0$$

Moreover, the rate of convergence of a sequence is quadratic if

$$\lim_{k\to\infty}\frac{\|v_{k+1}-v^*\|}{\|v_k-v^*\|^2} < C$$

for some positive constant C. From (17) it is easy to show that this condition holds for the sequence, $\left\{\lambda^{(k)}\right\}$, and hence it converges quadratically to λ^*.